



A new equation for dielectric permittivity of saturated soils based on polarization mechanics*

Ren-peng CHEN^{†1,2}, Yun-min CHEN^{†‡1,2}, Wei XU^{1,2}, Zhi-gang LIANG³, Wei FENG⁴

(¹MOE Key Laboratory of Soft Soils and Geoenvironmental Engineering, Zhejiang University, Hangzhou 310027, China)

(²Institute of Geotechnical Engineering, Zhejiang University, Hangzhou 310027, China)

(³Design Institute of Architecture of Hangzhou, Hangzhou 310001, China)

(⁴Lexmark International, Inc., Lexington, KY 40511, USA)

[†]E-mail: chenrp@zju.edu.cn; chenyunmin@zju.edu.cn

Received Dec. 12, 2007; revision accepted Dec. 20, 2007; published online Jan. 6, 2008

Abstract: Based on polarization mechanisms, such as electronic, ionic and orientational polarizations, a new equation for dielectric permittivity of soil is proposed to interpret the dielectric behavior of a mixture like soil, in terms of polarization process of its components and the interactions between its components. The dielectric permittivity is expressed in terms of a frequency-dependent part and a frequency-independent part. These two parts correspond to polarizations occurred at different frequency range. It is a new volumetric mixing model with theoretical background. Based on time domain reflectometry (TDR) measurements of saturated soil samples and test data from literature, comparisons of this model with some well established mixing models show that the curves for saturated sand soils and slurries resulted from the new equation, which agree well with TDR measurements, are close to those calculated from Birchak's model.

Key words: Dielectric permittivity, Saturated soils, Polarization, Time domain reflectometry (TDR)

doi:10.1631/jzus.A071620

Document code: A

CLC number: TU4

INTRODUCTION

As a mixture of different shaped granules, water and air, soil exhibits great complexity in many physical behaviors, including its dielectric characteristics, with regarding to its mineral composition, granular size distribution, water content, and porosity. The dielectric permittivity is one of the key parameters showing the dielectric behavior of a material. The dielectric behavior of soils and rocks is drawing more interest due to its known correlation to other soil properties like soil water content and porosity, with the advancement of electromagnetic measurement technologies, especially time domain reflectometry (TDR) and ground penetration radar (GPR). Many

studies have attempted to relate the permittivity of soil to the permittivities of its components. Various mixture equations have been published for soil with different ranges of application. There are two categories of such equations. The first category is empirical equations for determining water content and/or soil density (Wobschall, 1977; Topp *et al.*, 1980; Siddiqui and Drnevich, 1995; Yu and Drnevich, 2004; ASTM D6780-05, 2005). The second category is classified as volumetric mixing models, which are derived from discrete capacitor network theories or continuum mean field theories (Friedman *et al.*, 2006). Volumetric mixing models relate the effective dielectric permittivity of dielectric mixtures to their constituents' volumetric fractions and single-phase permittivities. A series of such models can be found in (Maxwell-Garnett, 1904; Looyenga, 1965; Birchak *et al.*, 1974; Dobson *et al.*, 1985; Heimovaara, 1994;

[‡] Corresponding author

* Project (Nos. 50278087 and 50308026) supported by the National Natural Science Foundation of China

Sihvola, 1999; Hilhost *et al.*, 2000). The influence of geometrical and interfacial factors on the effective permittivity were analyzed by Sen *et al.*(1981), Robinson and Friedman (2001; 2002; 2003; 2005), and Friedman *et al.*(2006).

A new equation for dielectric permittivity of saturated soils and rocks is developed in this paper based on polarization mechanisms. The frequency-dependent dielectric permittivity of a single-phase constituent is derived from various polarization mechanisms. Then the dielectric behavior of saturated soils and rocks is interpreted in terms of polarization process of its components and the interactions between its components. Comparisons of this model with some well established mixing models show the validity of the new equation.

THEORY

When an electric field is applied upon a dielectric, polarization occurs. Positive and negative bound charges move locally relatively to each other in response to the applied field. Therefore, net charge appears on the dielectric surface, with one side showing a positive net charge and the other a negative net charge. These charges are not free charges, but charges bounded within the dielectric that has become polarized. If the electric field is time varying, polarization is a dynamic phenomenon. It follows that polarization \mathbf{P} is proportional to the electric field \mathbf{E} in amplitude, but not necessarily in phase. A frequency-dependent complex permittivity $\varepsilon = \varepsilon' + j\varepsilon''$ is used to capture both amplitude and phase information.

Any condition or mechanism that renders the restrained relative displacement of charges can be considered as a polarization mechanism. For a homogeneous single-phase dielectric, three types of polarization mechanisms may be experienced: electronic, ionic and orientational polarizations. These three polarizations manifest at ultraviolet frequencies ($f_i \approx 10^7$ GHz, f_r is the relaxation frequency), infrared frequencies ($f_i \approx 10^4$ GHz) and microwave frequencies ($f_i \approx 10^2 \sim 10^{11}$ GHz), respectively (Fig.1).

If a dielectric is composed of N molecules of the same type per unit volume, the polarization under an applied electric field may be written as (Ramo *et al.*, 1994):

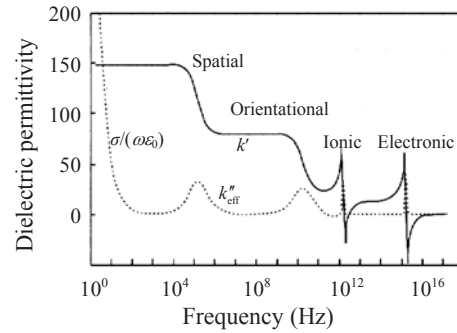


Fig.1 Dielectric permittivity for a hypothetical dielectric as a function of frequency w.r.t. polarization mechanisms (Santamarina *et al.*, 2001)

$$\mathbf{P} = \varepsilon_0 \chi \mathbf{E}_{\text{ex}} = N \alpha_{\text{T}} \mathbf{E}_{\text{loc}}, \quad (1)$$

where ε_0 is the permittivity of free space (vacuum), χ is the electric susceptibility, α_{T} is the molecular polarizability, \mathbf{E}_{ex} is the external field applied on the dielectric, and \mathbf{E}_{loc} is the Lorentz local field, which is defined in the following section.

The molecular polarizability has contributions from different polarization mechanisms. Therefore, we have

$$\alpha_{\text{T}} = \alpha_{\text{e}} + \alpha_{\text{i}} + \alpha_{\text{o}}, \quad (2)$$

where α_{e} , α_{i} and α_{o} is electronic, ionic, and orientational polarizability, respectively.

The effective frequency ranges of TDR and GPR are 0~10 GHz (Heimovaara *et al.*, 1996) and 25~1500 MHz (Powers, 1997), respectively. Hence, we can rewrite Eq.(2) as:

$$\alpha_{\text{T}} = \alpha_{\infty} + \alpha_{\text{f}}, \quad (3)$$

where α_{∞} represents the constant polarizability when $f > 10^4$ GHz, i.e., electronic and ionic polarizabilities; α_{f} is the frequency-dependent polarizability when $f < 10$ GHz, i.e., orientational and spatial polarizabilities.

In turn, we can express the total polarization as the sum of the constant polarization \mathbf{P}_{∞} which always follows the applied electric field instantly, and the frequency-dependent polarization $\mathbf{P}_{\text{f}}(f)$:

$$\mathbf{P} = \mathbf{P}_{\text{f}}(f) + \mathbf{P}_{\infty}. \quad (4)$$

The electric flux density vector \mathbf{D} is defined as:

$$\mathbf{D} = \varepsilon_0 \mathbf{E}_{\text{ex}} + \mathbf{P}. \quad (5)$$

Combining Eqs.(1) and (5) yields

$$\mathbf{D} = \varepsilon_0(1 + \chi) \mathbf{E}_{\text{ex}} = \varepsilon \mathbf{E}_{\text{ex}} = \varepsilon_r \varepsilon_0 \mathbf{E}_{\text{ex}}, \quad (6)$$

where ε is known as the permittivity of the dielectric, and ε_r is the relative permittivity or dielectric constant.

Clausius-Mossotti relation is known as (Lorrain and Corson, 1980):

$$(\varepsilon_r - 1)/(\varepsilon_r + 2) = N\alpha_r / (3\varepsilon_0). \quad (7)$$

Furthermore, when the frequency approaches to infinity, based on Eq.(3), we have

$$(\varepsilon_\infty - 1)/(\varepsilon_\infty + 2) = N\alpha_\infty / (3\varepsilon_0), \quad (8)$$

where ε_∞ is the relative dielectric permittivity when frequency approaches to infinity.

Combining Eqs.(1), (4) and (8), we derive the expression for \mathbf{P}_∞ :

$$\mathbf{P}_\infty = 3\varepsilon_0 \mathbf{E}_{\text{loc}} (\varepsilon_\infty - 1)/(\varepsilon_\infty + 2). \quad (9)$$

LORENTZ LOCAL FIELD AND EXTERNAL FIELD

Lorentz local field is defined as the electric field acting on the location of the molecule. The local field \mathbf{E}_{loc} is not necessarily identical to the external field \mathbf{E}_{ex} , but surely may be expressed as a superposition of the external field and some field introduced by the surrounding particles. The relationship between Lorentz local field \mathbf{E}_{loc} and external field \mathbf{E}_{ex} is given by (von Hippel, 1954)

$$\mathbf{E}_{\text{loc}} = \mathbf{E}_{\text{ex}} (\varepsilon_r + 2)/3. \quad (10)$$

When the electric field is applied on the single-phase dielectric, the external field \mathbf{E}_{ex} will equal to the applied field \mathbf{E}_0 . Thus,

$$\mathbf{E}_{\text{loc}} = \mathbf{E}_0 (\varepsilon_r + 2)/3. \quad (11)$$

When the electric field is applied on a mixture

like soil, the external field \mathbf{E}_{ex} is not always equal to the applied field \mathbf{E}_0 . By solving Laplace's equation with proper boundary conditions, the external field acting on one certain dielectric of the mixture $\mathbf{E}_{\text{ex}i}$ is given by (Ramo et al., 1994)

$$\mathbf{E}_{\text{ex}i} = 3\varepsilon_r \mathbf{E}_0 / (\varepsilon_{ri} + 2\varepsilon_r), \quad (12)$$

where ε_r and ε_{ri} are the permittivities of the mixture and the i th constituent within the mixture, respectively. Thus, the local field here is given by

$$\mathbf{E}_{\text{loc}i} = \frac{\varepsilon_{ri} + 2}{3} \mathbf{E}_{\text{ex}i} = \frac{\varepsilon_{ri} + 2}{3} \cdot \frac{3\varepsilon_r}{\varepsilon_{ri} + 2\varepsilon_r} \mathbf{E}_0. \quad (13)$$

NEW EQUATION FOR RELATIVE PERMITTIVITY OF SOILS

Relative permittivity of single-phase dielectric

As discussed in the previous section, with an applied electric field, the total polarization incurred within a dielectric consists of a frequency-dependent part, which reflects the effect of orientational polarization with longer relaxation time, and a frequency-independent part, which represents the effects of ionic and electronic polarizations with shorter relaxation time. The latter part relates to the relative permittivity at very high frequency (ε_∞), as shown in Eq.(9). Furthermore, we explore the relationship between $\mathbf{P}(f)$ and ε_r through loading analysis of dipole charges.

The separation of centers of positive and negative charges due to polarization phenomena can be modeled as an equivalent electric dipole composed of equal and opposite charges of q separated by a distance of l . The movement of either charge from the original position due to the applied field incurs the dipole moment \mathbf{P} , which is defined as

$$\mathbf{P} = ql. \quad (14)$$

In a dielectric which consists of molecules of the same type, the polarization vector \mathbf{P} is defined as the dipole moment per unit volume

$$\mathbf{P} = N_d ql, \quad (15)$$

where N_d is the number of dipoles per unit volume. If

the dipole is composed of a charge with heavier mass and an opposite charge with lighter mass, the motion of lighter charge dominates. We model this dipole moment with the motion of the charge with lighter mass of m .

The charge is subjected to electric force and magnetic force, and also affected by a restore force from the opposite charge, if any movement occurs. Therefore, the force acting on lighter charge q is:

$$F = -q(E_{loc} + v \times B_0) + ks, \tag{16}$$

where E_{loc} is the local field on the charge, v is the average mobile velocity of the charge, B_0 is the applied magnetic induction field, k is the linear factor of restore force, and s is the displacement of the charge. Taking the law of inertia into account, the force in x direction can be written as

$$F_x = m \frac{\partial^2 s_x}{\partial t^2} = -q(E_{locx} + v_y B_{0z}) + ks_x = -q \left(E_{locx} + \frac{\partial s_y}{\partial t} B_{0z} \right) + ks_x, \tag{17}$$

where E_{locx} is the local field in x direction on the charge, m is the mass of the charge, v_y is the average mobile velocity of the charge in y direction, s_x and s_y is displacement of the charge in x direction and y direction, respectively. The force in y direction can be written as the similar expression:

$$F_y = m \frac{\partial^2 s_y}{\partial t^2} = -q(E_{locy} + v_x B_{0z}) + ks_y = -q \left(E_{locy} + \frac{\partial s_x}{\partial t} B_{0z} \right) + ks_y. \tag{18}$$

Since the velocity of the charge in z direction is parallel to the magnetic induction field B_0 , the magnetic force will equal to zero. Hence the force in z direction can be written as

$$F_z = m \frac{\partial^2 s_z}{\partial t^2} = -qE_{locz} + ks_z. \tag{19}$$

If an electric field of a sinusoidal source with circular frequency ω is applied, the operator $\partial/\partial t$ may

be substituted by multiplying $j\omega$, where j is $\sqrt{-1}$. Then Eqs.(17)-(19) can be written as

$$\begin{cases} s_x = \frac{q(\omega+k/(m\omega)) \cdot E_{locx} - j\omega_c E_{locy}}{m \omega(\omega+k/(m\omega))^2 + \omega \cdot \omega_c^2} \\ s_y = \frac{q(\omega+k/(m\omega)) \cdot E_{locy} - j\omega_c E_{locx}}{m \omega(\omega+k/(m\omega))^2 + \omega \cdot \omega_c^2}, \\ s_z = \frac{qE_{locz}}{(\omega^2+k)m}, \end{cases} \tag{20}$$

where $\omega_c = qB_0/m$.

Note that in Eq.(20), when the frequency approaches to infinity, it results in

$$s_x = s_y = s_z = 0, \tag{21}$$

which indicates that the polarization incurred by the displacement maps to the first part of the total polarization in Eq.(4), $P_f(f)$. Therefore

$$P_f(f) = N_d q s, \tag{22}$$

Combining Eqs.(4), (5), (9), (16) and (21) yields

$$\begin{bmatrix} D_x \\ D_y \\ D_z \end{bmatrix} = \begin{bmatrix} \epsilon_0 E_{0x} + P_x \\ \epsilon_0 E_{0y} + P_y \\ \epsilon_0 E_{0z} + P_z \end{bmatrix} = \epsilon_0 \begin{bmatrix} E_{0x} \\ E_{0y} \\ E_{0z} \end{bmatrix} + \begin{bmatrix} P_{fx} \\ P_{fy} \\ P_{fz} \end{bmatrix} + \begin{bmatrix} P_{\infty x} \\ P_{\infty y} \\ P_{\infty z} \end{bmatrix} = \begin{bmatrix} \epsilon_0 E_{0x} + \frac{N_d q^2}{m} \cdot \frac{(\omega+k/(m\omega))E_{locx}}{\omega(\omega+k/(m\omega))^2 + \omega \cdot \omega_c^2} + 3\epsilon_0 \frac{\epsilon_\infty - 1}{\epsilon_\infty + 2} E_{locx} - j \frac{N_d q^2}{m} \cdot \frac{\omega_c}{\omega} \cdot \frac{E_{locx}}{(\omega+k/(m\omega))^2 + \omega_c^2} - j \frac{N_d q^2}{m} \cdot \frac{\omega_c}{\omega} \cdot \frac{E_{locy}}{(\omega+k/(m\omega))^2 + \omega_c^2} + 3\epsilon_0 \frac{\epsilon_\infty - 1}{\epsilon_\infty + 2} E_{locy} + \epsilon_0 E_{0y} + \frac{N_d q^2}{m} \cdot \frac{(\omega+k/(m\omega))E_{locy}}{\omega(\omega+k/(m\omega))^2 + \omega \cdot \omega_c^2} \\ \epsilon_0 E_{0z} + \frac{N_d q^2}{m} \cdot \frac{1}{\omega^2 + k} E_{locz} + 3\epsilon_0 \frac{\epsilon_\infty - 1}{\epsilon_\infty + 2} E_{locz} \end{bmatrix} = \begin{bmatrix} \epsilon_{rx} E_{0x} \\ \epsilon_{ry} E_{0y} \\ \epsilon_{rz} E_{0z} \end{bmatrix}. \tag{23}$$

If there is no applied magnetic field, Eq.(23) can

be written as

$$\begin{bmatrix} \epsilon_0 E_{0x} + \frac{N_d q^2}{(m\omega^2+k)} E_{locx} + 3\epsilon_0 \frac{\epsilon_\infty - 1}{\epsilon_\infty + 2} E_{locx} \\ \epsilon_0 E_{0y} + \frac{N_d q^2}{(m\omega^2+k)} E_{locy} + 3\epsilon_0 \frac{\epsilon_\infty - 1}{\epsilon_\infty + 2} E_{locy} \\ \epsilon_0 E_{0z} + \frac{N_d q^2}{(m\omega^2+k)} E_{locz} + 3\epsilon_0 \frac{\epsilon_\infty - 1}{\epsilon_\infty + 2} E_{locz} \end{bmatrix} = \epsilon_0 \begin{bmatrix} \epsilon_{rx} E_{0x} \\ \epsilon_{ry} E_{0y} \\ \epsilon_{rz} E_{0z} \end{bmatrix} \quad (24)$$

Substituting Eq.(11) into Eq.(24) leads to

$$\begin{bmatrix} \epsilon_0 E_{0x} + \frac{N_d q^2}{(m\omega^2+k)} \cdot \frac{\epsilon_{rx} + 2}{3} E_{0x} + 3\epsilon_0 \frac{\epsilon_\infty - 1}{\epsilon_\infty + 2} \cdot \frac{\epsilon_{rx} + 2}{3} E_{0x} \\ \epsilon_0 E_{0y} + \frac{N_d q^2}{(m\omega^2+k)} \cdot \frac{\epsilon_{ry} + 2}{3} E_{0y} + 3\epsilon_0 \frac{\epsilon_\infty - 1}{\epsilon_\infty + 2} \cdot \frac{\epsilon_{ry} + 2}{3} E_{0y} \\ \epsilon_0 E_{0z} + \frac{N_d q^2}{(m\omega^2+k)} \cdot \frac{\epsilon_{rz} + 2}{3} E_{0z} + 3\epsilon_0 \frac{\epsilon_\infty - 1}{\epsilon_\infty + 2} \cdot \frac{\epsilon_{rz} + 2}{3} E_{0z} \end{bmatrix} = \epsilon_0 \begin{bmatrix} \epsilon_{rx} E_{0x} \\ \epsilon_{ry} E_{0y} \\ \epsilon_{rz} E_{0z} \end{bmatrix} \quad (25)$$

For a single-phase homogeneous and isotropic dielectric, the relative permittivities in three directions are the same, i.e., $\epsilon_r = \epsilon_{rx} = \epsilon_{ry} = \epsilon_{rz}$. Finally we can obtain the new equation for the permittivity of single-phase dielectric from Eq.(25):

$$\frac{\epsilon_r - 1}{\epsilon_r + 2} = \frac{1}{3\epsilon_0} \frac{N_d q^2}{m\omega^2 + k} + \frac{\epsilon_\infty - 1}{\epsilon_\infty + 2} \quad (26)$$

From Eq.(26), the relative permittivity can be expressed by two parts. The first part is frequency-dependent. Considering that the linear factor for the restore force k is changing with temperature, this part is temperature dependent as well. The second part is frequency-independent, reflecting the effects of electronic and ionic polarizations, which have very fast relaxation time.

It is necessary to point out that in Eq.(23) and later, m is the statistical average of the mass of the dipole charge, k is also the statistical average of the factor of restore force. We make an assumption that the dipoles in a dielectric can be described as an

equivalent number of identical dipoles with the same dipole mass and factor of restore force. Here the number of dipoles per unit volume N_d is substituted by the equivalent number of identical dipoles per unit volume N_{eq} .

Relative permittivity of multi-phase dielectric

For one certain constituent within the multi-phase dielectric, the local field is given by Eq.(13). Substituting Eq.(13) into (24) yields

$$\begin{bmatrix} \epsilon_0 E_{0x} + \frac{N_{di} q^2}{(m_i \omega^2 + k_i)} \cdot \frac{\epsilon_{rxi} + 2}{3} \cdot \frac{3\epsilon_{rx}}{\epsilon_{rxi} + 2\epsilon_{rx}} E_{0x} + 3\epsilon_0 \frac{\epsilon_\infty - 1}{\epsilon_\infty + 2} \cdot \frac{\epsilon_{rxi} + 2}{3} \cdot \frac{3\epsilon_{rx}}{\epsilon_{rxi} + 2\epsilon_{rx}} E_{0x} \\ \epsilon_0 E_{0y} + \frac{N_{di} q^2}{(m_i \omega^2 + k_i)} \cdot \frac{\epsilon_{ryi} + 2}{3} \cdot \frac{3\epsilon_{ry}}{\epsilon_{ryi} + 2\epsilon_{ry}} E_{0y} + 3\epsilon_0 \frac{\epsilon_\infty - 1}{\epsilon_\infty + 2} \cdot \frac{\epsilon_{ryi} + 2}{3} \cdot \frac{3\epsilon_{ry}}{\epsilon_{ryi} + 2\epsilon_{ry}} E_{0y} \\ \epsilon_0 E_{0z} + \frac{N_{di} q^2}{(m_i \omega^2 + k_i)} \cdot \frac{\epsilon_{rzi} + 2}{3} \cdot \frac{3\epsilon_{rz}}{\epsilon_{rzi} + 2\epsilon_{rz}} E_{0z} + 3\epsilon_0 \frac{\epsilon_\infty - 1}{\epsilon_\infty + 2} \cdot \frac{\epsilon_{rzi} + 2}{3} \cdot \frac{3\epsilon_{rz}}{\epsilon_{rzi} + 2\epsilon_{rz}} E_{0z} \end{bmatrix} = \epsilon_0 \begin{bmatrix} \epsilon_{rx} E_{0x} \\ \epsilon_{ry} E_{0y} \\ \epsilon_{rz} E_{0z} \end{bmatrix} \quad (27)$$

where N_{di} is the number of dipoles per unit volume of the i th constituent. For the multi-phase dielectric as a whole, Eq.(27) can be written as Eq.(25), where ϵ_r is the relative permittivity of this multi-phase dielectric.

Note that m_i and k_i is statistical average for dipole charge mass and factor of restore force of the i th constituent, respectively. Assuming that different constituents have dipoles with similar lighter mass and also comparable factor of restore force, we have:

$$m_i \omega^2 + k_i = m_j \omega^2 + k_j = \dots = \bar{m} \omega^2 + \bar{k} \quad (28)$$

Here the number of dipoles per unit volume of the i th constituent N_{di} is substituted by the equivalent number of identical dipoles per unit volume of the constituent N_{eq} . Eq.(27) can be written as

$$\begin{aligned}
 & \left[\begin{aligned}
 & \varepsilon_0 E_{0x} + \frac{N_{eq} q^2}{(m\omega^2 + k)} \cdot \frac{\varepsilon_{rxi} + 2}{3} \cdot \frac{3\varepsilon_{rx}}{\varepsilon_{rxi} + 2\varepsilon_{rx}} E_{0x} + \\
 & 3\varepsilon_0 \frac{\varepsilon_\infty - 1}{\varepsilon_\infty + 2} \cdot \frac{\varepsilon_{rxi} + 2}{3} \cdot \frac{3\varepsilon_{rx}}{\varepsilon_{rxi} + 2\varepsilon_{rx}} E_{0x} \\
 & \varepsilon_0 E_{0y} + \frac{N_{eq} q^2}{(m\omega^2 + k)} \cdot \frac{\varepsilon_{ryi} + 2}{3} \cdot \frac{3\varepsilon_{ry}}{\varepsilon_{ryi} + 2\varepsilon_{ry}} E_{0y} + \\
 & 3\varepsilon_0 \frac{\varepsilon_\infty - 1}{\varepsilon_\infty + 2} \cdot \frac{\varepsilon_{ryi} + 2}{3} \cdot \frac{3\varepsilon_{ry}}{\varepsilon_{ryi} + 2\varepsilon_{ry}} E_{0y} \\
 & \varepsilon_0 E_{0z} + \frac{N_{eq} q^2}{(m\omega^2 + k)} \cdot \frac{\varepsilon_{rzi} + 2}{3} \cdot \frac{3\varepsilon_{rz}}{\varepsilon_{rzi} + 2\varepsilon_{rz}} E_{0z} + \\
 & 3\varepsilon_0 \frac{\varepsilon_\infty - 1}{\varepsilon_\infty + 2} \cdot \frac{\varepsilon_{rzi} + 2}{3} \cdot \frac{3\varepsilon_{rz}}{\varepsilon_{rzi} + 2\varepsilon_{rz}} E_{0z}
 \end{aligned} \right] \\
 & = \varepsilon_0 \begin{bmatrix} \varepsilon_{rx} E_{0x} \\ \varepsilon_{ry} E_{0y} \\ \varepsilon_{rz} E_{0z} \end{bmatrix}. \tag{29}
 \end{aligned}$$

The *i*th constituent occupies a volume fraction v_i of the mixture. The mixture contains n constituents, with the sum of all volume fractions equals one. The contribution of this *i*th constituent to the number of equivalent dipoles per unit volume N_{eq} of the mixture is $N_{eq} v_i$. The number of equivalent dipoles per unit volume is the sum of contributions from all constituents. Therefore, we have

$$N_{eq} = \sum_{i=1}^n N_{eq} v_i, \quad \sum_{i=1}^n v_i = 1. \tag{30}$$

Combining Eqs.(25), (26), (28), (29) and (30) yields the new equation for permittivity of multi-phase dielectric:

$$\left(2 \sum_i A_i - 3 \right) \varepsilon_r^2 + \left(\sum_i A_i \varepsilon_{ri} + 4 \sum_i A_i + 3 \right) \varepsilon_r + 2 \sum_i A_i \varepsilon_{ri} = 0, \tag{31}$$

where $A_i = v_i(\varepsilon_{ri} - 1)/(\varepsilon_{ri} + 2)$.

Eq.(31) shows that the relative permittivity of a dielectric mixture can be calculated if the relative permittivity and relative volume of each component are given. There is no additional assumption needed for this calculation. Theoretically, this equation should be applicable for any dielectric mixture like soil. The following sections are to exam the validity of this theory.

TESTING METHODS AND MATERIALS

The new equation for dielectric permittivity of mixture, Eq.(31), is evaluated with test results from soil samples of standard sand, Hangzhou fluvial sand and Hangzhou clay.

The fluvial sand samples were air-dried and ground to pass 0.5 or 0.25 mm sieve respectively to obtain medium or fine sand sample. Selected properties of the samples are presented in Table 1.

The soil samples were placed in the test cylinder and boiled for half an hour to one hour until they were saturated. Let the sample deposits until the surface water becomes clear, and then drain the surface water, measure the volume and weight of the soil sample in order to calculate its porosity. Three to seven different porosities were achieved for each soil sample by applying vibration.

TDR measurements were carried out with Campbell Scientific TDR100 with a step voltage pulse having a rise-time of about 200 ps. Two TDR probes were used: one is a three-rod probe, with rod length of 10.7 cm, rod diameter of 0.3 cm and rod-to-rod distance of 1.14 cm; the other is six-rod probe (one at the center and five equally spaced rods around the perimeter) with rod length of 12 cm, rod diameter of 0.3 cm and rod-to-rod space of 2 cm.

The apparent dielectric constant of each soil specimen K_a was obtained from the TDR measurement by determining the first reflection at the surface of the specimen and the second reflection from the end of the probe. It is calculated as Eq.(32):

Table 1 Selected properties of soil samples

Sample	Texture	Clay (%)	Fine sand (%)	Medium sand (%)	Coarse sand (%)	Gravel (%)	Specific gravity
Standard sand	Sand	0	35	5	50	10	2.63
Fine sand	Sand	0	100	0	0	0	2.71
Medium sand	Sand	0	0	100	0	0	2.70
Hangzhou clay	Clay	100	0	0	0	0	2.73

$$K_a = [ct/(2L)]^2, \quad (32)$$

where L is the length of the probe rod, t is the time difference between the two reflections and c is the light speed in free space.

The relationship between ε_r and K_a calculated from TDR measurement was discussed by Heimovaara (1994). K_a is a quantity dependent on the TDR measurement system as well as data processing, and is considered to be close to the real part of the relative permittivity at the high end of the frequency range for the TDR measurement system. Therefore, by using K_a from a TDR measurement, the result only corresponds to the relative permittivity at a certain frequency, which is tied to the frequency range of the TDR measurement system. The same limitation also applies to other relative permittivity models verified by TDR measurements.

RESULTS AND DISCUSSION

Application of models

The models most commonly in use are equations found by Birchak *et al.* (1974) and Topp *et al.* (1980). An important group of published mixture equations is based on the "exponential model"

$$\varepsilon_r^\alpha = \sum_{i=1}^n v_i \varepsilon_{ri}^\alpha, \quad (33)$$

where the exponent α is an empirical constant. This mixture equation is often used in Soil Science. For $\alpha=0.5$, Eq.(33) is Birchak's model. The value of α was proposed by many researchers (Wang, 1980; Dobson *et al.*, 1985; Whalley, 1993; Heimovaara 1994; Robinson and Friedman, 2002).

Another popular equation is Topp's calibration model (Topp *et al.*, 1980). Topp's calibration curve is a broadly accepted calibration equation for volumetric water content measurement using TDR. Topp's equation is shown in Eq.(34):

$$\varepsilon_r = 3.03 + 9.3\theta + 146\theta^2 - 76\theta^3, \quad (34)$$

where θ is the volumetric water content of soil.

Another classical model for biphasic dielectric is Maxwell-Garnett model:

$$\frac{\varepsilon_r - \varepsilon_e}{\varepsilon_r + 2\varepsilon_e} = v_{in} \frac{\varepsilon_{in} - \varepsilon_e}{\varepsilon_{in} + 2\varepsilon_e}, \quad (35)$$

where ε_e is the permittivity of one dielectric as environment while ε_{in} is the permittivity of the other dielectric as inclusion, v_{in} is the volume fraction of the inclusion.

Results from the TDR experiments on the soil samples were used to examine the new equation along with the abovementioned models. Since saturated soil specimens were used, there are only two components, soil granule and water. For the soil granule, a value of 5.0 is used as the relative permittivity ε_{rs} , based on the estimates for sedimentary rocks and quartz. For water, a value of 81.0 is used as ε_{rw} at room temperature of 20 °C (Topp *et al.*, 1980). In addition, in Maxwell-Garnett model, the soil granule is treated as inclusion while the water as environment.

Comparison with some existing models

Measured apparent dielectric constant (ε_r) vs porosity (e) for saturated sands and saturated slurries (a clay soil with high void ratio) is shown in Figs.2a and 2b, respectively. Fig.2 shows the corresponding curve of the new equation and those of Birchak's model, Topp's equation and Maxwell-Garnett's model.

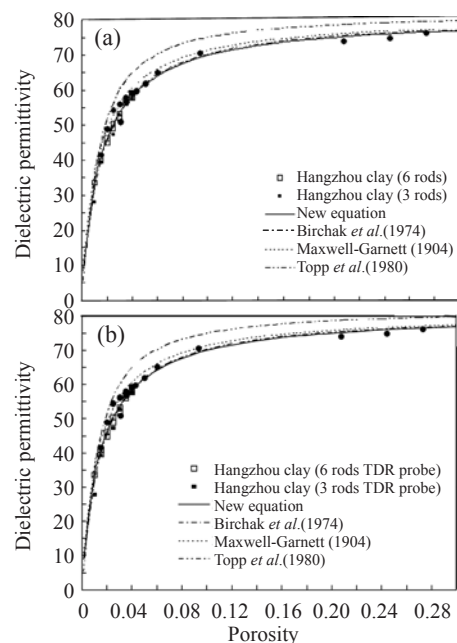


Fig.2 Dielectric permittivity ε_r as function of soil porosity e for saturated sands (a) and slurries (b)

The Birchak's model provided a satisfactory fit of data. Nevertheless, there is evidence that value of α in Eq.(33) should be treated as an empirical fitting parameter (White *et al.*, 1994). Hilhorst *et al.*(2000) suggested that reasonable fit of Eq.(33) with $\alpha=0.5$ to experimental data for soils can be only accidental. For soils, an equation with larger number of fitting parameters is needed to give a statistically satisfactory fit to data. Dobson *et al.*(1985) determined α by regression from data for frequencies from 4 to 18 GHz and soil types ranging from sandy loam to silty clay, and obtained a value of 0.65. Roth *et al.*(1990) found the optimum value of α for several soils equal to 0.46.

The Topp's equation appears to be a satisfactory model for coarse-textured soils. This result is similar to the findings of other authors. Dirksen and Dasberg (1993) found Eq.(34) to be suitable for soils with specific surface up to 100 m²/g and bulk density from 1350 to 1500 kg/m³.

The curve of Maxwell-Garnett model is not equally in accordance with our measurements. This is a dispersion model describing the macroscopic effects of the interactions of the dispersed particles with their immediate surroundings. It was found that this model cannot describe the complex dielectric permittivities measured at lower frequencies. Heimovaara *et al.*(1994) interpreted that the dispersion model was developed for higher frequency (>500 MHz), where interface effects do not play a role.

Fig.2 shows that curves for saturated sand soils and slurries resulted from the new equation, which agree well with TDR measurements, are close to those calculated from Birchak's model. It can be explained by the fact that the new equation is of the same family as the volumetric refractive model.

A further discussion of the derivation of the new equation shows its essential relationship with the exponential model. For the case that each molecule of different constituents in the mixture experiences the same applied electric field, $E_{loc}=E_0$, we will find the same equation as Silberstein's model (Silberstein, 1895),

$$\varepsilon_r = \sum_{i=1}^n v_i \varepsilon_{ii} . \quad (36)$$

Eq.(36) is the case that if the mixture contains no microscopic bodies with surfaces at which electric

field refractions can take place. In Silberstein's model the polarization of each molecule is the direct result of the applied electric field. However, a mixture often contains clusters, permanently or temporarily, of one constituent, which are equivalent to microscopic bodies. Thus the permittivities calculated from this model will be greater than those from measurements.

For the case that the external field equals the applied field, which means the interactions between constituents are neglected, the new equation can be written as

$$(\varepsilon_r + 2)^{-1} = \sum_{i=1}^n v_i (\varepsilon_{ii} + 2)^{-1} . \quad (37)$$

Eq.(37) also belongs to the family of the volumetric refractive mixing model and provides a lower bound of the new equation.

The model of Sen *et al.*(1981) is derived for a self-similar medium of infinitely wide particle size distribution:

$$[(\varepsilon_1 - \varepsilon_{eff})/(\varepsilon_1 - \varepsilon_0)](\varepsilon_0 / \varepsilon_{eff})^{1/3} = n. \quad (38)$$

Eq.(38) means that smaller particles of permittivity ε_1 are mixed into the background of permittivity ε_0 .

Note that for saturated sands and slurries, the amount of bound water is little and then its contribution to soil permittivity is negligible. The permittivity of bound water is lower than that of free water. For simplicity, the effects of bound water are not discussed in this study. However, the expression of the new equation shows that it can include more constituents, such as air and bound water.

Data from Friedman's experiment was applied for further validation of the new equation. Fig.3 shows the comparison of the dielectric permittivity ε_{eff} of water-saturated binary mixture with its porosity. The binary mixture is composed of small glass spheres (45~53 μm) and large ones (450~500 μm) of similar solid permittivity. The curve resulted from the new equation model for a solid with a permittivity of $\varepsilon_1=6.75$ immersed in water with a permittivity of $\varepsilon_w=78.5$ agrees well with the TDR measurements. The Maxwell-Garnett's model Eq.(35) and the self-similar model Eq.(38) form the upper and lower bounds to the measurements. The permittivity of the mixed medium obtained by the new equation, only

depends on the relative permittivity and relative volume of each component and gives an acceptable accuracy. With the consideration of size distribution and particle shape, the mixing model always gives good matching with the test data. However, the size distribution and particle shape are difficult to be found for the varieties of the soil type.

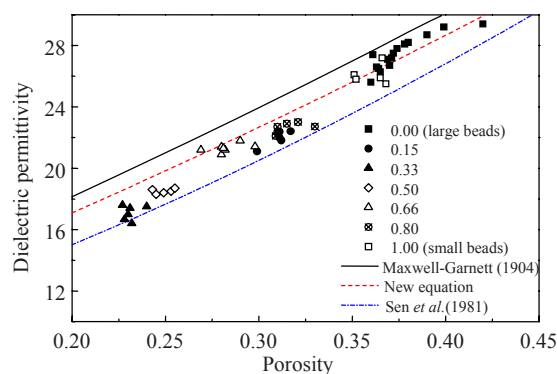


Fig.3 Comparison of the dielectric permittivity of binary mixture of glass beads with presented new equation. Test data points are from friedman's experiment

CONCLUSION

Different polarization mechanisms contribute to the total polarization of a dielectric material with an applied electric field. Three polarization mechanisms are most significant, namely, electronic, ionic and orientational polarizations. These three polarizations manifest effects in different frequency range. With a frequency range of concern (<10 GHz), the total polarization consists of a constant part and a frequency-dependent part. The electronic and ionic polarizations mainly contribute to the constant part, and orientational polarization to the other. The orientational polarization is modeled with a motion analysis of dipole particles. A theoretical interpretation of the relative permittivity in terms of polarization mechanism is derived for a single-phase dielectric and a multi-phase dielectric.

A volumetric mixing model is also established based on the same theory of polarization mechanism. Unlike most mixing models which are empirical without solid theoretical background, this model provides not only reasonable agreement with test data and other accepted models, but also consideration of

the polarization process with few assumptions. The results from this model are in accordance with those of Birchak's model, with an analysis showing that the new model has essential relationship with the exponential model.

Based on TDR measurements on sand and slurry specimens and test data from literature, the validity and usability of this volumetric mixing model are verified. Although the TDR results can only provide a partial verification of the value for relative dielectric permittivity with the calculation of apparent dielectric constant, they are effective to exam the plausibility of a volumetric mixing model.

ACKNOWLEDGMENTS

The authors are grateful to Dr. V. P. Drnevich for his suggestions.

References

- ASTM D6780-05, 2005. Standard Test Method for Water Content and Density of Soil in Place by Time Domain Reflectometry (TDR). West Conshohocken, PA.
- Birchak, J.R., Gardner, C.G., Hipp, J.E., Victor, J.M., 1974. High dielectric constant microwave probes for sensing soil moisture. *Proc. IEEE*, **62**:93-98.
- Dirksen, C., Dasberg, S., 1993. Improved calibration of time domain reflectometry for soil water content measurements. *Soil Sci. Soc. Am. J.*, **57**:660-667.
- Dobson, M.C., Ulaby, F.T., Hallikainen, M.T., El-Rayes, M.A., 1985. Microwave dielectric behaviour of wet soil, part II: dielectric mixing models. *IEEE Transactions on Geoscience and Remote Sensing*, **GE-23**(1):35-46. [doi:10.1109/TGRS.1985.289498]
- Friedman, S.P., Robinson, D.A., Jones, S.B., 2006. Review of Geometrical and Interfacial Factors Determining the Effective Permittivity-volumetric Water Content Relationships of Soil and Rocks. Proceedings of the 3rd International Symposium and Workshop on Time Domain Reflectometry for Innovative Soils Applications, Purdue University.
- Heimovaara, T.J., 1994. Frequency domain analysis of time domain reflectometry waveforms 1: Measurement of the complex dielectric permittivity of soils. *Water Resources Research*, **30**(2):189-199. [doi:10.1029/93WR02948]
- Heimovaara, T.J., Bouten, W., Verstraten, J.M., 1994. Frequency domain analysis of time domain reflectometry waveforms 2: A four-component complex dielectric mixing model for soils. *Water Resources Research*, **30**(2):201-209. [doi:10.1029/93WR02949]
- Heimovaara, T.J., de Winter, E.J.G., van Loon, W.K.P., Esveld, D.C., 1996. Frequency-dependency dielectric permittiv-

- ity from 0 to 1 GHz: time domain reflectometry measurements compared with frequency domain network analyzer measurements. *Water Resources Research*, **32**(12):3603-3610. [doi:10.1029/96WR02695]
- Hilhorst, M.A., Dirksen, C., Kampers, F.W.H., Feddes, R.A., 2000. New dielectric mixture equation for porous materials based on depolarization factors. *Soil Sci. Soc. Am. J.*, **64**:1581-1587.
- Looyenga, H., 1965. Dielectric constant of heterogeneous mixtures. *Physica*, **31**(3):401-406. [doi:10.1016/0031-8914(65)90045-5]
- Lorrain, P., Corson, D.R., 1980. *Electromagnetic Fields and Waves*. Freeman, W.H., San Francisco, p.504-535.
- Maxwell-Garnett, J.C., 1904. Colours in metal glasses and metal films. *Trans. Royal Society, London*, **203**(1):385-420. [doi:10.1098/rsta.1904.0024]
- Powers, M.H., 1997. Modeling frequency-dependent GPR. *The Leading Edge*, **16**(11):1657-1662. [doi:10.1190/1.1437549]
- Ramo, S., Whinnery, J.R., van Duzer, T., 1994. *Fields and Waves in Communication Electronics* (3rd Ed.). John Wiley, New York, p.187-220.
- Robinson, D.A., Friedman, S.P., 2001. The effect of particle size distribution on the effective dielectric permittivity of saturated granular media. *Water Resources Research*, **37**(1):33-40. [doi:10.1029/2000WR900227]
- Robinson, D.A., Friedman, S.P., 2002. The effective permittivity of dense packings of glass beads, quartz sand and their mixtures immersed in different dielectric backgrounds. *J. Non-crystalline Solids*, **305**(1-3):261-267. [doi:10.1016/S0022-3093(02)01099-2]
- Robinson, D.A., Friedman, S.P., 2003. A method for measuring the solid particle permittivity or electrical conductivity of rocks, sediments, and granular materials. *J. Geophys. Res.*, **108**(B2):2076. [doi:10.1029/2001JB000691]
- Robinson, D.A., Friedman, S.P., 2005. Electrical conductivity and dielectric permittivity of sphere packing: measurements and modelling of cubic lattices, randomly packed monosize spheres and multi-size mixtures. *Physica A: Statistical Mechanics and its Applications*, **358**(2-4):447-465. [doi:10.1016/j.physa.2005.03.054]
- Roth, K., Schulin, R., Fluehler, H., Attinger, W., 1990. Calibration of TDR for water content measurement using a composite dielectric approach. *Water Resources Research*, **26**(10):2267-2273. [doi:10.1029/90WR01238]
- Santamarina, J.C., Klein, K.A., Fam, M.A., 2001. *Soils and Waves*. John Wiley & Sons Ltd., West Sussex, UK.
- Sen, P.N., Scala, C., Cohen, M.H., 1981. A self-similar model for sedimentary rocks with application to the dielectric constant of fused glass beads. *Geophysics*, **46**(5):781-795. [doi:10.1190/1.1441215]
- Siddiqui, S.I., Drnevich, V.P., 1995. Use of Time Domain Reflectometry for the Determination of Water Content and Density of Soil. FHWA/IN/JHRP-95/9, Purdue University, West Lafayette.
- Sihvola, A., 1999. *Electromagnetic Mixing Formulas and Applications*. Institution of Electrical Engineers, Herts, Stevenage, UK.
- Silberstein, L., 1895. Untersuchungen über die Dielectricitätsconstanten von Mischungen und Lösungen. *Annalen der Physik und Chemie*, **292**(12):661-679. [doi:10.1002/andp.18952921204]
- von Hippel, R., 1954. *Dielectric Materials and Applications*. The MIT Press, Cambridge.
- Topp, G.C., Davis, J.L., Annan, A.P., 1980. Electromagnetic determination of soil water content: measurements in coaxial transmission lines. *Water Resources Research*, **16**:574-582.
- Wang, J.R., 1980. The dielectric properties of soil-water mixtures at microwave frequencies. *Radio Science*, **15**:977-985.
- Whalley, W.R., 1993. Considerations on the use of time-domain reflectometry (TDR) for measuring soil water content. *European Journal of Soil Science*, **44**(1):1-9. [doi:10.1111/j.1365-2389.1993.tb00429.x]
- White, I., Knight, J.H., Zegelin, S.J., Topp, G.C., 1994. Comments on "Considerations on the use of time-domain reflectometry (TDR) for measuring soil water content" by W.R. Whalley. *European Journal of Soil Science*, **45**(4):503-508. [doi:10.1111/j.1365-2389.1994.tb00536.x]
- Wobschall, D., 1977. A theory of the complex dielectric permittivity of soil containing water: the semidisperse model. *IEEE Trans. on Geoscience Electronics*, **15**(1):49-58. [doi:10.1109/TGE.1977.294513]
- Yu, X., Drnevich, V.P., 2004. Soil water content and dry density by time domain reflectometry. *Journal of Geotechnical and Geoenvironmental Engineering*, **130**(9):922-934. [doi:10.1061/(ASCE)1090-0241(2004)130:9(922)]